# The importance of different timings of excitatory and inhibitory pathways in neural field models

**Carlo R. Laing***
**Institute of Information and Mathematical Sciences, Massey University, Private Bag 102-904 North Shore Mail Centre, Auckland, New Zealand**
**and**
**S. Coombes†**
**Department of Mathematical Sciences, University of Nottingham, Nottingham, NG7 2RD, UK.**

**December 15, 2005**

**Running title: "Different timings in neural field models"**

**Corresponding author:**
**Carlo R. Laing,**
**Institute of Information and Mathematical Sciences,**
**Massey University, Private Bag 102-904 North Shore Mail Centre,**
**Auckland, New Zealand**
**ph: +64-9-4140800 extn 41038**
**fax: +64-9-441-8136**
**email: c.r.laing@massey.ac.nz**

*email: c.r.laing@massey.ac.n
†email: stephen.coombes@nottingham.ac.uk

# The importance of different timings of excitatory and inhibitory pathways in neural fields models

**Abstract**

In this paper we consider a neural field model comprised of two distinct populations of neurons, excitatory and inhibitory, for which both the velocities of action potential propagation and the time courses of synaptic processing are different. Using recently-developed techniques we construct the Evans function characterising the stability of both stationary and travelling wave solutions, under the assumption that the firing rate function is the Heaviside step. We find that these differences in timing for the two populations can cause instabilities of these solutions, leading to, for example, stationary breathers. We also analyse "anti-pulses," a novel type of pattern for which all but a small interval of the domain (in moving coordinates) is active. These results extend previous work on neural fields with space-dependent delays, and demonstrate the importance of considering the effects of the different time-courses of excitatory and inhibitory neural activity.

## 1 Introduction

Models of neural fields have been studied extensively over the last few decades [5, 19, 32, 33, 13, 30, 6, 7], in the hope that they will provide information about possible macroscopic patterns of activity in the cortex. These patterns are on a much larger spatial scale than that of individual neurons, so the models take a continuum limit in which space is continuous and the mean firing rate of neurons is the variable of interest. Among some of the patterns of interest are stationary, spatially-localised "bumps" of activity [1, 33, 30]. These are thought to be involved in working memory and feature selectivity in the visual system [19]. Travelling waves of activity are also of interest. Experimentally, these can be induced by stimulating pharmacologically treated neural tissue slices [20, 32]; they have also been observed in several different areas of the cortex of awake animals, often when no stimulation is present [10]. An important question is: Given a neural model, what sorts of spatiotemporal patterns can exist and which features of the model are important in determining the existence and stability of these patterns? In this paper we answer these questions, concentrating on delays and differences in timing relating to neural processing.

It is well-known that different types of synaptic events have quite different time-courses. For example, inhibitory $GABA_A$ synapses decay with a time constant of approximately 15ms, while excitatory NMDA synapses have a time constant of approximately 80ms [27]. Also, the speed of propagation of an action potential along an axon depends on the diameter of the axon, as well as whether it is myelinated or not [27]. Measured axonal conduction velocities in the cortex can differ by a factor of 10, depending on the type of neuron examined, and can be as low as $1 m/s$ [38]. These velocities are also use-dependent and can change over time [37]. Interestingly, anaesthetics have been shown to increase conduction velocity in myelinated fibres — the consequences of this are discussed in [40]. In this paper we study a neural field model that explicitly includes differences in timing (in both the speed of synaptic processing and the conduction speed) for two populations of neurons, excitatory and inhibitory.

Many authors modelling neural systems have assumed instantaneous communication between different parts of the domain [19, 33, 13, 30], but recently the effects of delays due to finite conduction speeds and synaptic processing have been investigated. Some of these more recent studies have involved rate models, in which the firing rate of neurons is the variable of interest [6, 7, 32, 22, 21], while several others have investigated networks of spiking neurons [2, 15, 17]. In all of these papers only on

solutions in Sec. 4. In both cases we use an Evans function approach [7] to determine the stability of solutions and the conditions necessary for both drift and breathing bifurcations. In Sec. 5 we examine the collision of two fronts, which leads us to study anti-pulses. We also brie y consider networks in which excitatory connections have longer spatial range than inhibitory ones. We nish with a discussion in Sec. 6.

## 2 The model

We analyze a neural eld model with synaptic activity $u = u_e(x, t) - u_i(x,$

## 2.1 A PDE description

For the particular choice of synaptic footprint (4) it is possible to obtain an equivalent PDE description of the integral equation (2), using ideas developed by Jirsa and Haken [23]. To see this we write

$$\psi_a(x,t) = \int_{-\infty}^{\infty}\int_{-\infty}^{\infty} G_a(x-y,t-s)\rho(y,s)\,ds\,dy, \tag{5}$$

where

$$G_a(x,t) = \delta(t-|x|/v_a)w_a(x) \tag{6}$$

and we use the notation $\rho(x,t) = f\circ u(x,t)$. Introducing Fourier transforms of the following form

$$\psi_a(x,t) = \frac{1}{(2\pi)^2}\int_{-\infty}^{\infty}\int_{-\infty}^{\infty} e^{-i(kx+\omega t)}\psi_a(k,\omega)dkd\omega, \tag{7}$$

allows us to write

$$\psi_a(k,\omega) = G_a(k,\omega)\rho(k,\omega). \tag{8}$$

It is straightforward to show that the Fourier transform of (6) is

$$G_a(k,\omega) = \nu_a(\omega/v_a + k) + \nu_a(\omega/v_a - k), \tag{9}$$

where

$$\nu_a(E) = \int_0^{\infty} w_a(x)e^{-iEx}dx = \left(\frac{\Gamma_a}{2\sigma_a}\right)\frac{1}{\sigma_a^{-1}+iE}. \tag{10}$$

We have using (9) and (10) that

$$G_a(k,\omega) = \frac{\Gamma_a(1+i\omega/\omega_a)}{(1+i\omega/\omega_a)^2+\sigma_a^2k^2}, \tag{11}$$

where $\omega_a = v_a/\sigma_a$. We may now write (8) as

$$\left\{(1+i\omega/\omega_a)^2+\sigma_a^2k^2\right\}\psi_a(k,\omega) = \Gamma_a\left(1+i\omega/\omega_a\right)\rho(k,\omega), \tag{12}$$

which upon inverse Fourier transforming gives the PDE:

$$\partial_{tt}\psi_a + \left(\omega_a^2 - v_a^2\partial_{xx}\right)\psi_a + 2\omega_a\partial_t\psi_a = \Gamma_a\left(\omega_a^2+\omega_a\partial_t\right)\rho. \tag{13}$$

If we choose the synaptic response $\eta_a(t)$ to be the exponential: $\eta_a(t) = \alpha_a\Theta(t)\exp(-\alpha_a t)$, where $\Theta(t)$ is the Heaviside function, de ned by $\Theta(t) = 1$ for $t \geq 0$ and zero otherwise, we can also write the integral equation (1) as the differential equation

$$\frac{1}{\alpha_a}\frac{\partial u_a}{\partial t} = -u_a(x,t) + \psi_a(x,t) \tag{14}$$

In numerical simulations of the model we integrate (13) and (14) using nite difference approximations to the spatial derivatives and work with the choice

$$f(u) = \frac{1}{1+e^{-\beta(u-h)}}, \tag{15}$$

where $h$ can be thought of as a threshold and $\beta$ as a gain parameter.

Note that if we set $v_e = v_i = v$ and $\eta_e = \eta_i = \eta$, i.e. we remove the differences in timings for the two neural populations, our system reduces to

$$u = \eta * \psi, \tag{16}$$

$$\psi(x,t) = \int_{-\infty}^{\infty} dy w(y) f\circ u(x-y, t-|y|/v) \tag{17}$$

where $w(y) \equiv$

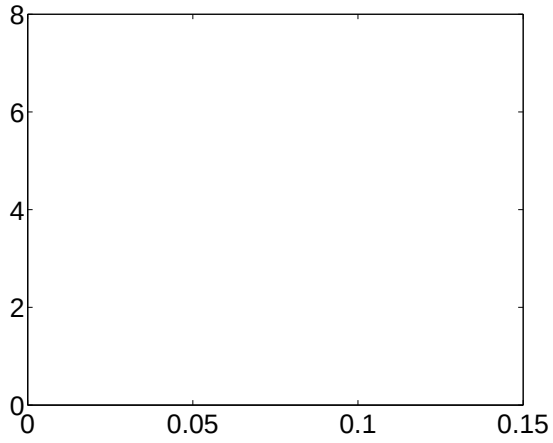
8
6
4
2
0
0
0.05
0.1
0.15

**3.2**

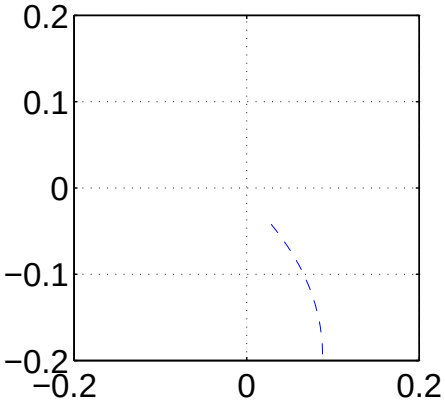
0.2
0.1
0
−0.1
−0.2
−0.2
0
0.2

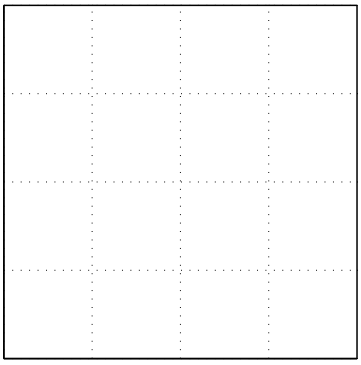

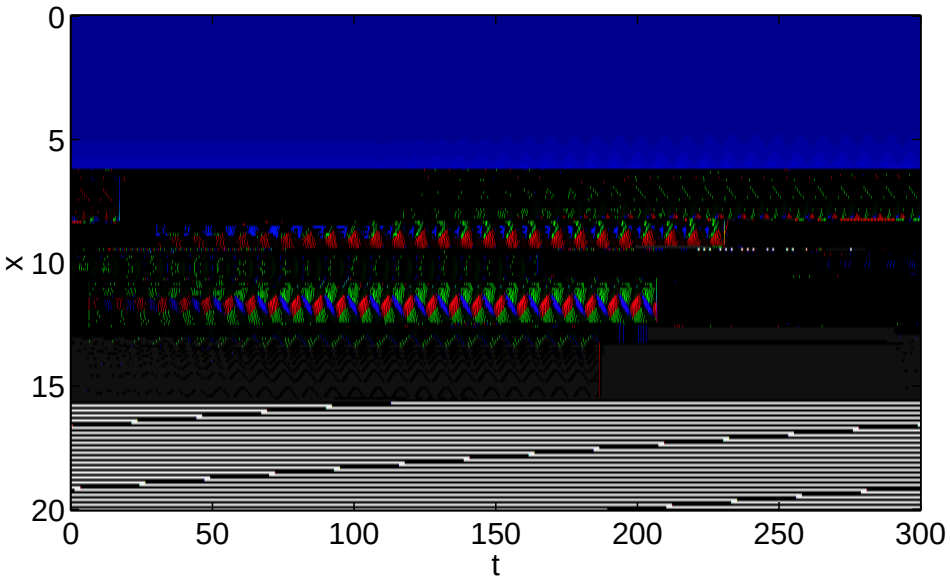


**Figure 7: Supercritical Hopf bifurcation of a stationary bump. At t = 100 we switched $v_e$ from 0.8 to 0.5 (and a small perturbation was added). 200 spatial points were used. Other parameters are $\sigma_e = 1, \sigma_i = 2, \alpha_i = 1.8, \alpha_e = 3, v_i = 1, h = 0.1, \Gamma = 1$. $u_e$ is plotted; red high, blue low.**

**obtain**

$$[w(\Delta)]^2 \left[1 - \cos\theta - (1/4)\sin^2\theta\right] = 0 \tag{28}$$

**which is only true if $\theta = 0, 2\pi, 4\pi \ldots$ Substituting these values of $\theta$ back into (27) we see that it cannot simultaneously be satis ed, i.e. $E(\lambda)$ has no purely imaginary roots. If $w(\Delta) = 0$ the only root of $E(\lambda)$ is $\lambda = 0$, which corresponds to the saddle-node bifurcation in Fig. 1. Thus both types of instabilities are a result of the differences in timings for the two populations.**

**Bifurcations of the types discussed in this section have recently been observed in a system with one neural population but in which the threshold is a dynamic variable [8]. There, the authors also saw a stationary bump start to move as an eigenvalue moved through zero, and stationary breathers caused by a supercritical Hopf bifurcation. Breathers have also been observed in neural eld equations by Bressloff et al. [4, 13], but in those papers the authors made the domain inhomogeneous, inducing a bump to occur over a spatially-localised input. During normal awake operation the cortex continuously receives inhomogeneous inputs, so the response of a neural model with such inputs is of interest. However, under general anaesthesia the cortex will receive less input (and conduction velocities may be increased [40]) so it is also of interest to study the existence and stability of patterns in this situation.**

**Blomquist et al. [1]Tj 29..4058lfnce**

**introduce the coordinate $\xi = x - ct$ and seek functions $U(\xi, t) = u(x - ct, t)$ that satisfy the full integral model equations. In the $(\xi, t)$ coordinates, these integral equations can be expressed as $U(\xi, t) =$**
**$U$** eB 1 Tf 0.12 0 0 -0.12 531 0 Td

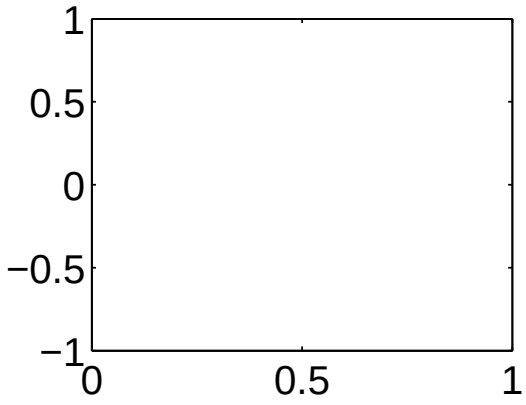
1
0.5
0
−0.5
−1
0
0.5
1

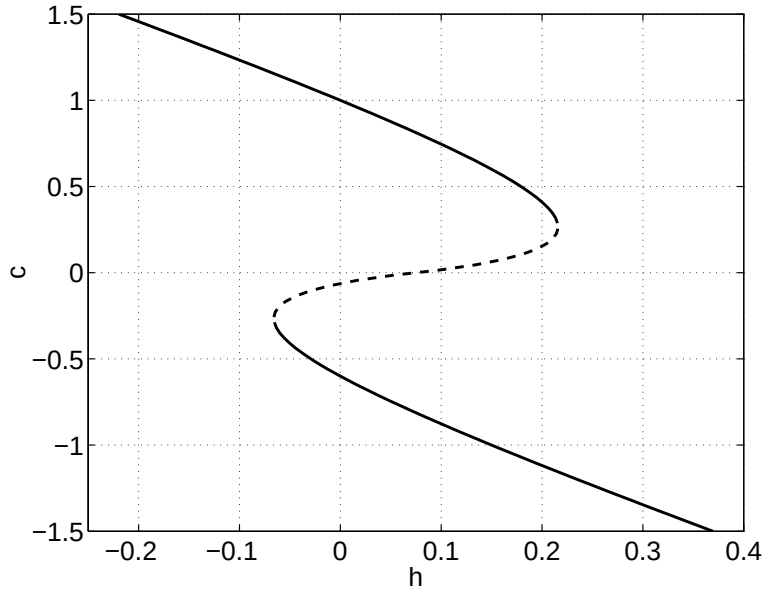


**Figure 9: Front speed as a function of h. Stable fronts are represented by solid lines, unstable by dashed. Parameters are $\Gamma = 0.85$, $\alpha_e = 1$, $\alpha_i = 0.1$, $v_e = v_i = 1$, $\sigma_i = 2$ and $\sigma_e = 1$.**

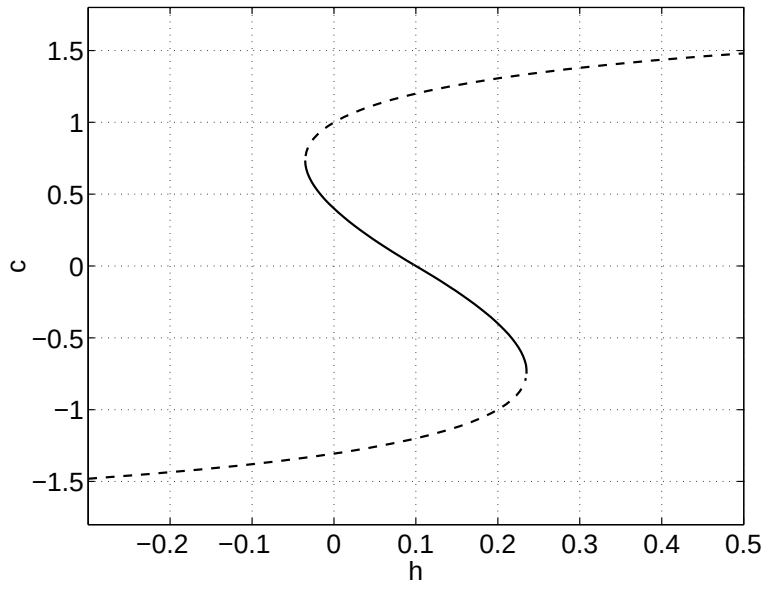


**Figure 10: Front speed as a function of h. Parameters are $\alpha_i = \alpha_e = 1, v_e = v_i = 1, \sigma_e = 1, \sigma_i = 2, \Gamma = 0.8$. The solid branch is stable, while the dashed ones are unstable.**

$$2h = 2(1-\Gamma) + 2\left[\Gamma \exp(-\alpha_i \Delta/c) - \exp(-\alpha_e \Delta/c)\right] + \left[\frac{\exp(-\alpha_e \Delta/c) - 1}{1 - c m_e^-/\alpha_e}\right] + \left[\frac{\exp(-\alpha_e \Delta/c) - \exp(-m_e^+ \Delta)}{1 - c m_e^+/\alpha_e}\right] - \Gamma\left[\frac{\exp(-\alpha_i \Delta/c) - 1}{1 - c m_i^-/\alpha_i}\right] - \Gamma\left[\frac{\exp(-\alpha_i \Delta/c) - \exp(-m_i^+ \Delta)}{1 - c m_i^+/\alpha_i}\right] \tag{41}$$

$$2h = \left[\frac{1 - \exp(m_e^- \Delta)}{1 - c m_e^-/\alpha_e}\right] - \Gamma\left[\frac{1 - \exp(m_i^- \Delta)}{1 - c m_i^-/\alpha_i}\right] \tag{42}$$

**Note that as $c \to 0$, both (41) and (42) reduce to the equation governing the width of a stationary bump, (20), as expected.**

**The Evans function takes the same form as in Sec. 3.2, with (21) replaced by**

$$A(\lambda) = \begin{bmatrix} A(0,\lambda) & B(0,\lambda) \\ A(\Delta,\lambda) & B(\Delta,\lambda) \end{bmatrix}. \tag{43}$$

**where $A(\xi,\lambda) = A_e(\xi,\lambda) - A_i(\xi,\lambda)$, $B(\xi,\lambda) = B_e(\xi,\lambda) - B_i(\xi,\lambda)$, and**

$$A_a(\xi,\lambda) = \frac{1}{c|q'(0)|}\int_{\xi/(1-c/v_a)}^{\infty} dy w_a(y)\eta_a(-\xi/c + y/c - y/v_a)e^{-\lambda(y-\xi)/c} \tag{44}$$

$$B_a(\xi,\lambda) = \frac{1}{c|q'(\Delta)|}\int_{(\xi-\Delta)/(1+c/v_a)}^{\infty} dy w_a(y)\eta_a((\Delta-\xi)/c + y/c - |y|/v_a)e^{-\lambda(y-(\xi-\Delta))}$$

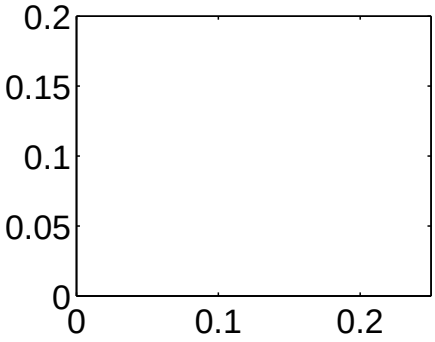
0.2
0.15
0.1
0.05
0
0
0.1
0.2

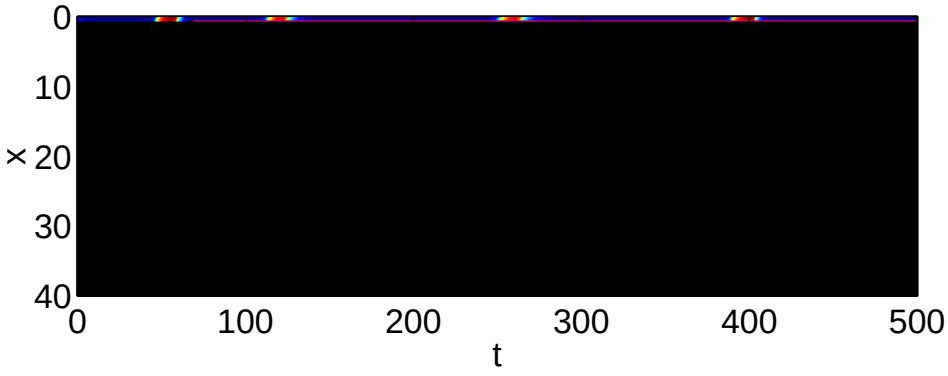


**Figure 13: A subcritical Hopf bifurcation of a moving pulse. At t = 100, h is switched from 0.05 to 0.07. $u_e$ is plotted, red high and blue low. Periodic boundary conditions are used. Other parameters are as in Fig. 12.**

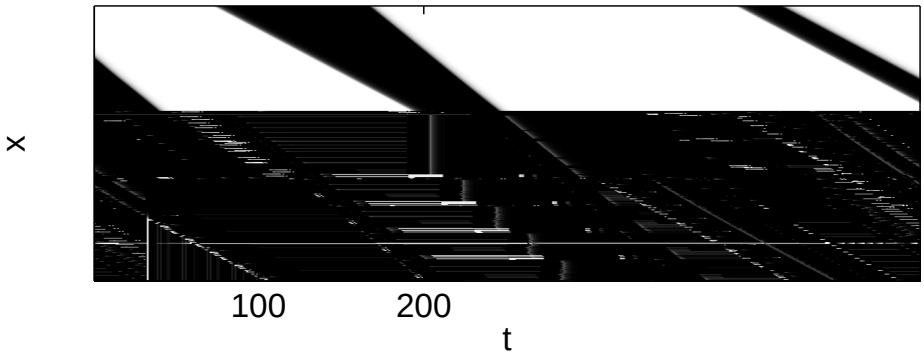

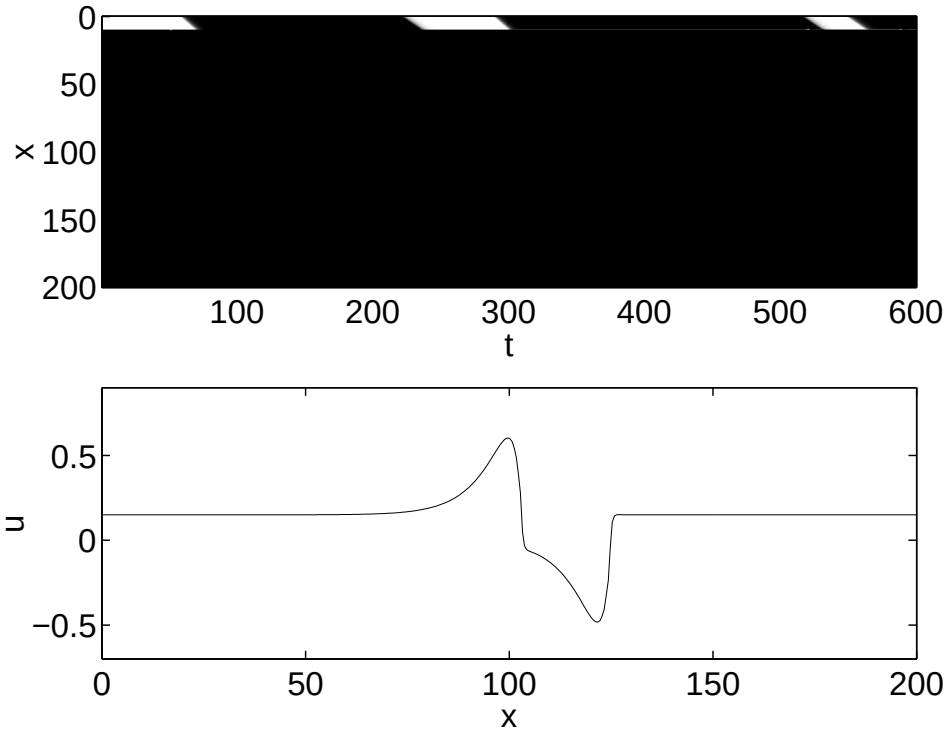


**Figure 15: A wide moving pulse for which the back travels slower than the front, leading to the formation of an "anti-pulse". Top: $u_e$ is plotted, with black being high and white low. Bottom: $u = u_e - u_i$ once the anti-pulse has formed. $h = 0.05$, so most of the domain is active. Other parameters are as in Fig. 9.**

## 5.1 Anti-pulses

For anti-pulses, $q(\xi) < h$ for $0 < \xi < \Delta$ and $q(\xi) > h$ otherwise. Using $\int_{-\infty}^{\infty} w_a(x)dx = \Gamma_a$, we have

$$\psi_a(\xi) = \begin{cases} \Gamma_a - F_a\left(\frac{-\xi}{1+c/v_a}, \frac{\Delta-\xi}{1+c/v_a}\right) & \xi \le 0 \\ \Gamma_a - F_a\left(0, \frac{\xi}{1-c/v_a}\right) - F_a\left(0, \frac{\Delta-\xi}{1+c/v_a}\right) & 0 < \xi < \Delta\,, \\ \Gamma_a - F_a\left(\frac{\xi-\Delta}{1-c/v_a}, \frac{\xi}{1-c/v_a}\right) & \xi \ge \Delta \end{cases} \tag{53}$$

where $F_a$ is given by (40). The conditions $q(0) = h = q(\Delta)$ are then easily determined using $q(\xi) = q_e(\xi) - q_i(\xi)$ and

$$q_a(\xi) = \int_0^{\infty} \eta_a(s)\psi_a(\xi + cs)ds \tag{54}$$

and the fact that these integrals have essentially been done in the determination of (41)-(42). They are

$$\begin{aligned} 2h \;=\; & -2\left[\Gamma \exp(-\alpha_i\Delta/c) - \exp(-\alpha_e\Delta/c)\right] \\ & - \left[\frac{\exp(-\alpha_e\Delta/c) - 1}{1 - cm_e^-/\alpha_e}\right] - \left[\frac{\exp(-\alpha_e\Delta/c) - \exp(-m_e^+\Delta)}{1 - cm_e^+/\alpha_e}\right] \\ & + \Gamma\left[\frac{\exp(-\alpha_i\Delta/c) - 1}{1 - cm_i^-/\alpha_i}\right] + \Gamma\left[\frac{\exp(-\alpha_i\Delta/c) - \exp(-m_i^+\Delta)}{1 - cm_i^+/\alpha_i}\right] \end{aligned} \tag{55}$$

and

$$2h = 2(1-\Gamma) - \left[\frac{1 - \exp(m_e^-\Delta)}{1 - cm_e^-/\alpha_e}\right] + \Gamma\left[\frac{1 - \exp(m_i^-\Delta)}{1 - cm_i^-/\alpha_i}\right] \tag{56}$$

The width and speed of anti-pulses is determined by the simultaneous solution of (55)-(56). The Evans function for antipulses has the same form as that for pulses, since

forSn

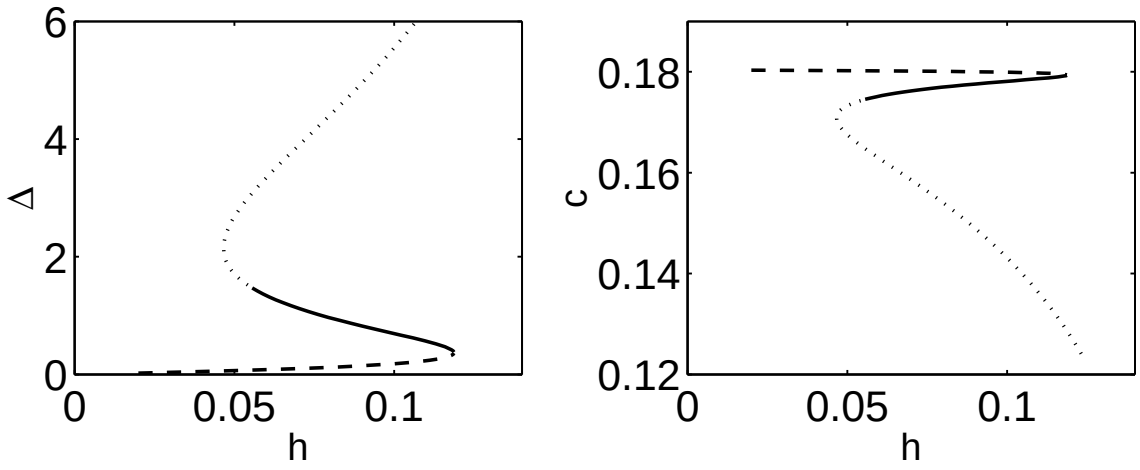


**Figure 16: Width (left panel) and speed (right panel) of a travelling pulse as a function of h, with inverted Mexican hat connectivity. Solid lines represent stable one-bump solutions and dashed unstable, while the dotted lines indicate a solution of (41)-(42) which is not a one-bump solution. Parameters are $v_e = 0.2$, $v_i = 1$, $\alpha_e = 1$, $\alpha_i = 1$, $\Gamma = 0.7$, $\sigma_e = 2$, $\sigma_i = 1$.**

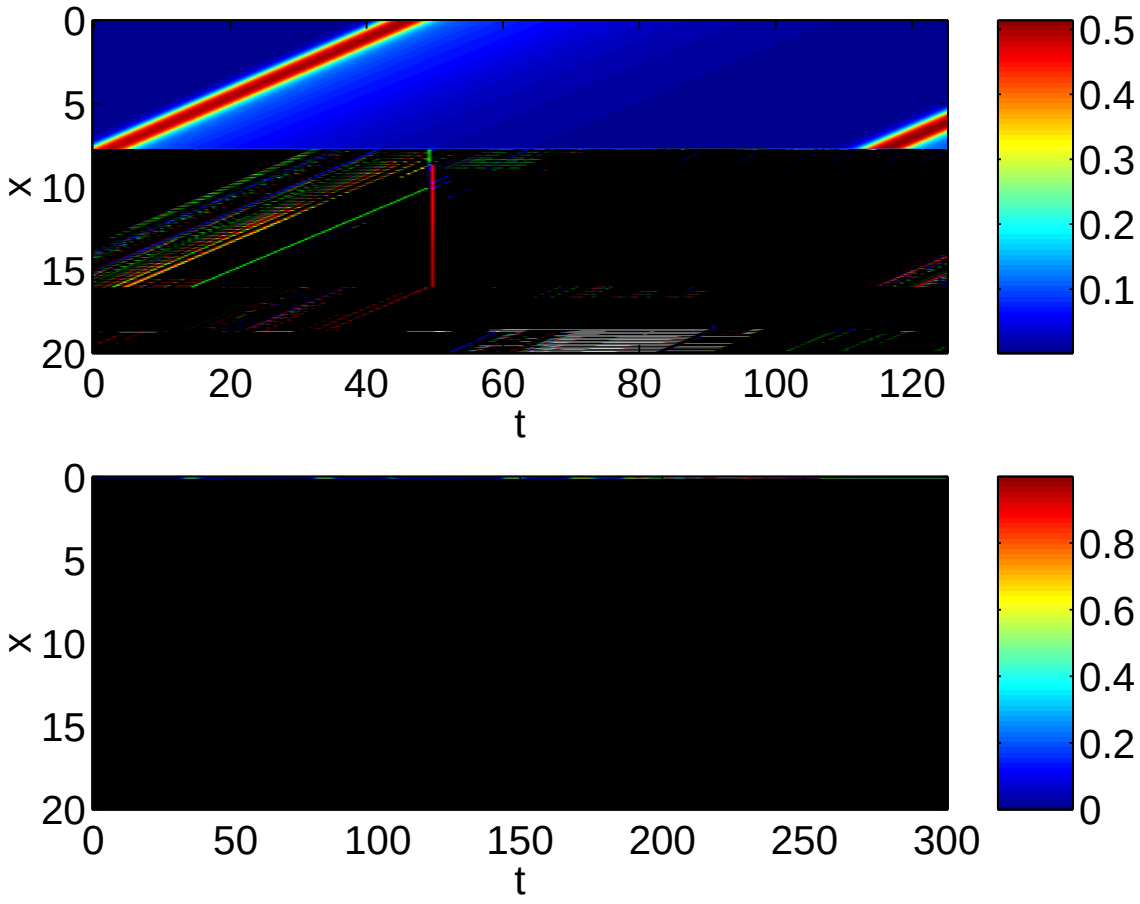


**Figure 17: Top: a stable travelling pulse for inverted Mexican hat connectivity. Bottom: the interaction of two such travelling pulses leads to**

breathing bumps. These bifurcations can be found by explicitly constructing an Evans function for these solutions and, as shown in Sec. 3.4, they cannot occur if the synaptic time-constants and conduction velocities are the same for both layers.

Our work has produced results similar to those of several other groups. For example, Curtu and Ermentrout [9] recently studied an extension of the system first discussed by Hansel and Sompolinsky [19]. This model had one neural population, Mexican-hat type connectivity, an adaptation variable and no delays. The authors found travelling and standing waves, and stationary, spatially-periodic patterns. However, their results were derived by linearising about the spatially-uniform state, and are thus unable to say anything regarding spatially-localised patterns of the type studied here.

Golomb and Ermentrout [15] studied the effects of delays on propagating activity. They included a fixed delay and found that increasing this led to lurching waves. (We did not include a fixed delay, but see below.) However, they used a spiking neural network in which each neuron could only fire once, and only excitatory coupling. Because of this, they could not find stationary or arbitrarily slowly moving patterns, as we have. In later work [16, 17] these authors studied a network with both excitatory and inhibitory populations but did not include conduction delays for most of their analysis, and still allowed neurons to fire at most once, thus precluding the existence of stationary patterns. One interesting result that they found was the coexistence of both fast and slow propagating pulses, which we have not found. However, these authors found that once neurons were allowed to fire multiple times this bistability disappeared, with only the slow pulses persisting.

Blomquist et al. [1] studied a two-layer neuronal network without delays (an extension of that studied by Pinto and Ermentrout [33]), and found both subcritical and supercritical Hopf bifurcations of stationary bumps. Coombes and Owen [8] studied a single neural layer with Mexican-hat connectivity and a variable representing spike frequency adaptation. They found both drifting and breathing bifurcations of stationary bumps, as we have, and also supercritical Hopf bifurcations of travelling bumps, which we have not found. We now discuss possible extensions of the work presented here.

One extension would be to break the homogeneity of the domain (reflected by the appearance of x and y in (2) in (both)(connectivitsaps.)T9Tj 15.7083 0mbin (adaptatand)Tj /R89 9.965se

nite conduction velocity does not destabilise travelling bumps or fronts in one spatial dimension [5, 15], it is not clear whether the same holds in two dimensions.

A more general model, more clearly differentiating the two neural populations, would be

$$u_a = \eta_a * \psi_a, \qquad a \in \{e, i\} \tag{59}$$

$$\psi_e(x,t) = \int_{-\infty}^{\infty} dy w_{ee}(y) f_e \circ u_e(x-y, t-|y|/v_e) - \int_{-\infty}^{\infty} dy w_{ie}(y) f_i \circ u_i(x-y, t-|y|/v_i) \tag{60}$$

$$\psi_i(x,t) = \int_{-\infty}^{\infty} dy w_{ei}(y) f_e \circ u_e(x-y, t-|y|/v_e) - \int_{-\infty}^{\infty} dy w_{ii}(y) f_i \circ u_i(x-y, t-|y|/v_i) \tag{61}$$

Here we not only have different conduction velocities $v_e$ and $v_i$ and different synaptic lters $\eta_e$ and $\eta_i$, but different ring rate functions $f_e$ and $f_i$ and four coupling functions, $w_{ee}, w_{ei}, w_{ie}$ and $w_{ii}$ instead of the two in (1)-(2). Choosing $f_a(u) = \Theta(u - h_a)$, i.e. using the Heaviside function as the ring rate function, with two different thresholds, we should be able to analyse (59)-(61) in much the same way as we have analysed (1)-(2) in this paper. Some of the analysis in [8], in which the threshold is a dynamical variable, may also be used

[9] R Curtu and B Ermentrout. Pattern formation in a network of excitatory and inhibitory cells with adaptation. SIAM Journal on Applied Dynamical Systems, 3:191–231, 2004.

[10] G B Ermentrout and D Kleinfeld. Traveling electrical waves in cortex: insights from phase dynamics and speculation on a computational role. Neuron, 29:33–44, 2001.

[11] G B Ermentrout and J B McLeod. Existence and uniqueness of travelling waves for a neural network. Proceedings of the Royal Society of Edinburgh, 123A:461–478, 1993.

[12] J Evans. Nerve axon equations: IV The stable and unstable impulse. Indiana University Mathematics Journal, 24:1169–1190, 1975.

[13] S E Folias and P C Bressloff. Breathing pulses in an excitatory neural network. SIAM Journal on Applied Dynamical Systems, 3:378–407, 2004.

[14] P S Goldman-Rakic. Cellular basis of working memory. Neuron, 14:477–485, 1995.

[15] D Golomb and G B Ermentrout. Effects of delay on the type and velocity of travelling pulses in neuronal networks with spatially decaying connectivity. Network: Computation in Neural Systems, 11:221–246, 2000.

[16] D Golomb and G B Ermentrout. Bistability in pulse propagation in networks of excitatory and inhibitory populations. Physical Review Letters, 86:4179–4182, 2001.

[17] D Golomb and G B Ermentrout. Slow excitation supports propagation of slow pulses in networks of excitatory and inhibitory populations. Physical Review E, 65:061911, 2002.

[18] S Guo, L Huang, and J Wu. Regular dynamics in a delayed network of two neurons with all-or-none activation functions. Physica D, 206:32–48, 2005.

[19] D Hansel and H Sompolinsky. Methods in neuronal modeling: from ions to networks, pages 499–567. MIT Press, Cambridge, MA, 1998.

[20] X Huang, W C Troy, Q Yang, H Ma, C R Laing, S J Schiff, and J Wu. Spiral waves in disinhibited mammalian neocortex. The Journal of Neuroscience, 24:9897–9902, 2004.

[21] A Hutt. Effects of nonlocal feedback on traveling fronts in neural elds subject to tranrtuisson

[31] B A McGuire, C D Gilbert, P K Rivlin, and T N Wiesel. Targets of horizontal connections in macaque primary visual cortex. Journal of Comparative Neurology, 305:370–392, 1991.

[32] D J Pinto and G B Ermentrout. Spatially structured activity in synaptically coupled neuronal networks: I. Travelling fronts and pulses. SIAM Journal on Applied Mathematics, 62:206–225, 2001.

[33] D J Pinto and G B Ermentrout. Spatially structured activity in synaptically coupled neuronal networks: II. Lateral inhibition and standing pulses. SIAM Journal on Applied Mathematics, 62:226–243, 2001.

[34] D J Pinto, R K Jackson, and C E Wayne. Existence and stability of traveling pulses in a continuous neuronal network. SIAM Journal on Applied Dynamical Systems, 4:954–984, 2005.

[35] A Roxin, N Brunel, and D Hansel. Role of delays in shaping spatiotemporal dynamics of neuronal activity in large networks. Physical Review Letters, 94:238103, 2005.

[36] L P Shayer and S A Campbell. Stability, bifurcation, and multistability in a system of two coupled neurons with multiple time delays. SIAM Journal on Applied Mathematics, 61:673–700, 2000.

[37] H A Swadlow. Physiological properties of individual cerebral axons studied in vivo for as long as one year. Journal of Neurophysiology, 54:1346–1362, 1985.

[38] H A Swadlow. Efferent neurons and suspected interneurons in s-1 forelimb representation of the awake rabbit: receptive elds and axonal properties. Journal of Neurophysiology, 63:1477–1498, 1990.

[39] N V Swindale. The development of topography in the visual cortex: a review of models. Network: Computation in Neural Systems, 7:161–247, 1996.

[40] N V Swindale. Neural synchrony, axonal path lengths and general anesthesia: A hypothesis. The Neuroscientist, 9:440–445, 2003.

[41] S Wiggins. Introduction to applied nonlinear dynamical systems and chaos. Springer-Verlag, New York, 1990.